Ultrasonics 96 (2019) 276–283

Contents lists available at ScienceDirect

Ultrasonics

journal homepage: www.elsevier.com/locate/ultras

Signal noise based transfer function approach for reliability estimation of ultrasonic inspection

Mohamed Subair Syed Akbar Ali[a,*], Anish Kumar[b], Prabhu Rajagopal[a]

[a] Center for Nondestructive Evaluation and Department of Mechanical Engineering, Indian Institute of Technology Madras, Chennai, Tamil Nadu, India
[b] Metallurgy and Materials Group, Indira Gandhi Centre for Atomic Research, Kalpakkam, Tamil Nadu, India

ARTICLE INFO

Keywords:
Transfer function
Ultrasonic testing
Probability of Detection (PoD)
Signal to noise ratio
Stainless steel

ABSTRACT

In recent years several methods for reducing the burden of experimentation for obtaining Probability of Detection (PoD) curves have been proposed, especially involving the use of numerical simulation. In particular, there is much interest in being able to estimate the PoD capabilities of a given NDE method, target embodiment and material, provided this is known for some canonical material for the same combination of method/embodiment. Ultrasonic experiments on materials with low signal to noise ratio (SNR) are often difficult and time consuming since the higher signal noise causes serious complications. Set in this context, this paper proposes an approach for transferring PoD curves among materials with different SNR values. The classical transfer function PoD approach is based on the hypothesis that the ratio of signals in related quadrants is equal, which requires large datasets for multiple quadrants. The approach proposed here directly deals with SNR instead of the ratio of signals, and thus requires only the experimental data of the parent application. The new approach is illustrated through example cases involving the prediction of PoD curves for ultrasonic inspection of an aluminium plate using the empirical PoD data for the same in austenitic stainless steel and mild steel. The approach is also demonstrated in each of the possible combinations among these three materials.

1. Introduction

The Probability of Detection (PoD) approach is today widely used for the assessment of reliability of Nondestructive Evaluation (NDE) techniques [1,2]. PoD curves are formally plotted as a function of characteristic defect dimensions and the values are dependent on uncertainties associated with the inspection technique as well as the defect configuration [3,4]. The classical signal response analysis method of PoD estimation [3] is based on the Maximum Likelihood Estimation (MLE) of linear regression over signal responses collected for a range of flaw sizes. As discussed in recent contributions [5], the mean of the linear regression of signal responses is thought to be related to intrinsic capabilities of the inspection system, while the variance arises from application parameters and human factors. As part of this 'modular approach', multi-parameter PoD models were proposed to adequately account for both the intrinsic capability and application parameters [6–9]. As human factors are among the significant sources of variance, several methods were also proposed to account for them explicitly [10–12]. More recently, a generalized PoD estimation procedure based on Weibull statistics (instead of Gaussian statistics assumed in the classical Berens [3] approach) was reported by the authors [13].

Despite such advances, PoD curve generation typically requires extensive experimental campaigns, which are expensive in terms of cost and time. Thus in recent years, researchers are focusing on reducing the cost of obtaining valid NDE reliability data. Over the last decade and more, initiatives such as the Model-Assisted Probability of Detection (MAPOD) in the USA [14] and PICASSO [15] project in Europe have considered replacing at least some of the experimental data required for PoD determination with results based on physics-based wave mechanical models. The authors have also recently presented work on Bayesian synthesis for simulation-assisted PoD curve generation [16].

PoD curves are dependent on factors specific to a given application: thus they need to be obtained for every new case or configuration, however similar they may be. Thus approaches for 'transferring' the PoD among various practical cases have been studied, commonly through the use of a transfer function [17–22]. In particular, a 'quadrant XFM approach' was demonstrated using various quadrants containing empirical data of real and artificial specimens with real and artificial flaws [18]. This 'classical' transfer function approach is based on the hypothesis that the ratio of signals in related quadrants is equal. The target PoD is estimated based on a linear regression model of PoD parameters for the other quadrants. Recently a similar attempt was

* Corresponding author.
E-mail address: zubair.musam@gmail.com (M.S. Syed Akbar Ali).

https://doi.org/10.1016/j.ultras.2018.09.015
Received 7 February 2018; Received in revised form 9 September 2018; Accepted 26 September 2018
Available online 29 September 2018
0041-624X/

reported based on the hypothesis that the ratio of the signals in simulations and experiments for a specific component is equal to the ratio of signals in related components [21]. A practical implementation of that approach to a high-frequency eddy current inspection for fatigue cracks was presented and numerical simulations were carried out using a semi-analytical software package [23]. A transfer function approach to predict the PoD curve for a high temperature application using low temperature ultrasonic measurements with the help of validated physics-based models has also been reported [22]. One of the key limitations of such model-based approaches is that since they are dependent on numerical results, the accuracy of underlying models is crucial.

In the work presented here, we develop a framework for transferring PoD curves for NDE of samples with different underlying materials, without employing simulations. In particular, we demonstrate the approach for ultrasonic NDE of specimen materials with low to high grain scattering-induced Signal to Noise Ratio (SNR). Ultrasonic experiments on materials with low SNR values are difficult in nature and more time consuming since the higher signal noise makes detection of defects challenging. SNR values for elastic waves in materials depend upon many variables including wave velocities, average grain size and distribution. In general, materials with different scattering factors (see [24] for example for discussion of scattering factors) will exhibit different levels of noise in ultrasonic signals. Hence our work focuses on developing a transfer function approach based on the signal noise in materials. We consider specimen samples made of two materials with a large difference in scattering factors, namely, Aluminium (Al) and Austenitic Stainless Steel (SS). Based on [24] for example, while Aluminium has a shear wave Rayleigh scattering factor of 86.5 dB/μsec. $(Mc/sec^4)\,cm^3$, SS is expected much to have much larger values, close to 3900 dB/μsec. $(Mc/sec^4)\,cm^3$. Additionally, a Mild Steel (MS) specimen is also considered for demonstration, which is expected to have a scattering factor close to 1500 dB/μsec. $(Mc/sec^4)\,cm^3$. Moreover, since a manual angle beam pulse-echo inspection scenario is considered for illustration, the above material choice also fulfills the requirement of equivalent wave velocities in the parent and target materials, in order to fix the procedural parameters [25] (wave mode, frequency, beam angle, etc.). Experiments were carried out on specimens with identical defect configurations. This work is confined to signal response $\hat{a}$ vs. a approach of PoD curve generation based on the classical Berens method guidelines [3].

This paper is organized as follows. Experiments are first described, including details of specimen samples and procedure adopted for independent trials. Our proposed signal noise based transfer function approach is then presented. Results obtained using this approach (with PoD transferred from empirical data for aluminium to SS and reverse) and their validation with fully empirical data are then presented. Discussion on the defect configurations in both parent and target materials is then presented, followed by a transfer PoD estimation for a MS specimen. Finally, the scope and limitations of this approach are discussed, followed, by conclusions and directions for further work.

2. Experiments

The proposed transfer function approach is demonstrated through the example case of PoD curve prediction for ultrasonic inspection of an aluminium specimen plate using empirical data from an austenitic SS plate of the same dimensions otherwise. Notches of 10 mm length (or transverse extent) and 3 mm width (or axial extent) were machined on a thick SS specimen in bottom-surface breaking configuration using the Electrical Discharge Machining (EDM) process. The notches are of different depths (or heights, in the bottom-surface breaking configuration) and their dimensions are given in Table 1. The photograph of the specimen is shown in Fig. 1 (shown reversed for better visualization).

Experiments using the conventional angle-beam technique (45° S-wave) were performed in the pulse-echo mode using a commercially available integrated probe with center frequency at 2 MHz [26]. A 3

Table 1
Dimensions of the EDM notches in the specimen.

Notch No.	A	B	C	D	E	F	G	H	I	J	K	L
Height (mm)	1	2	3	4	5	6	7	8	9	10	12	15

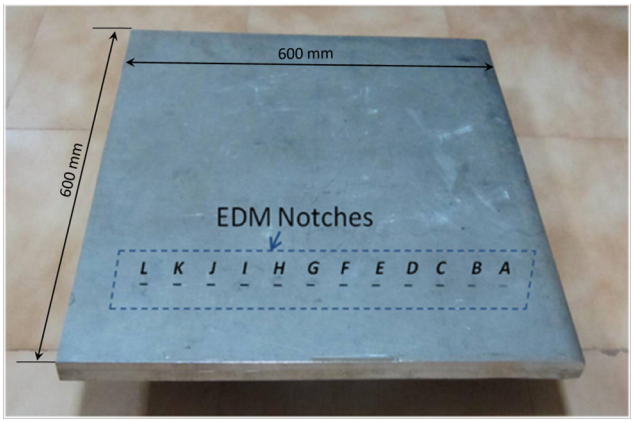

Fig. 1. Photograph showing stainless steel specimen sample plate with EDM notches of various heights (Labeled A-L).

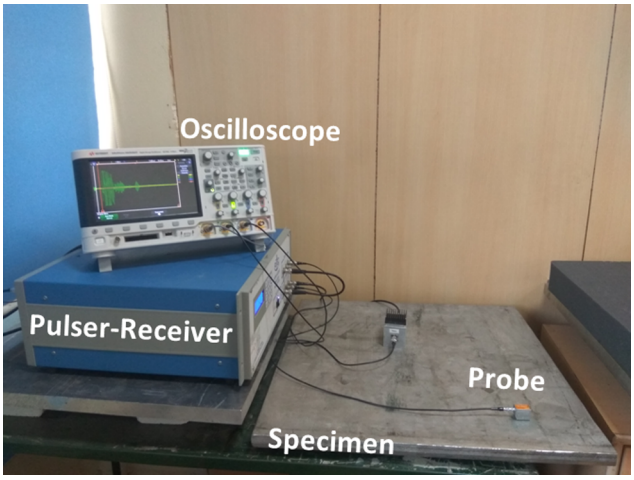

Fig. 2. Photograph showing the experimental setup.

cycle Hanning windowed toneburst from a RITEC 4000 pulser-receiver [27] was used to excite the probe, which was placed on the top surface of the plate, on a line perpendicular to and bisecting the notch lengthwise. The experimental setup is shown in Fig. 2. The probe position is optimized such that the maximum energy of the input signal is incident directly on the back-wall breaking corner of the notch. The output was received using an oscilloscope [28] and averaged over 512 ensembles to reduce random noise.

The uncertainties associated with measurements were accounted for by taking a statistically significant number (typically 30 for a normal distribution – see [13;29] for e.g. for more discussion of this point) of independent measurement trials for each notch case. After every trial the equipment is turned off and the setup including the connectors and couplant was dismantled. The complete setup is then recreated for fresh measurements to account for instrument uncertainties. The environmental noise was considered by switching off and on again the electrical appliances running in the background such as air-conditioning and also by performing the trials on different days.

For validation purposes, an aluminium specimen plate similar to the SS specimen was prepared with identically dimensioned and located EDM notches. Angle-beam pulse echo ultrasonic inspections were

carried out on the specimen and multiple independent measurements were taken, as described above.

3. Signal noise based transfer function

The transfer function approach we propose here, is essentially based on the hypothesis that the signals are linearly related to the defect (in this case, a crack) parameter which is (also) one of the primary assumptions in the classical (Berens) procedure for PoD computation [3]. The classical transfer function approach is actually based on a corollary of this linearity hypothesis where, the ratio of signals in related components is assumed to be equal [18,21]. In particular, the work reported in [21] assumes that the ratio of signals in aluminium is equal to the ratio of the signals in titanium plates and it was expressed as shown in the following equation,

$$\frac{y_i^{\exp,Ti}}{y_i^{sim,Ti}} = \frac{y_i^{trans,Al}}{y_i^{sim,Al}}, \quad i = 1. \ldots n \tag{1}$$

where y is the signal response and n is the number of observation points.

In this work ([21], quoted above), the equality of variability in the signal was adapted from [18], where the variability in experimental signals with the aluminium component is assumed as being equivalent to that in titanium. The transfer function was specified by the following relations,

$$\beta_0^{trans,Al} = \beta_0^{exp,Ti} + \beta_0^{sim,Al} - \beta_0^{sim,Ti} \tag{2}$$

$$\beta_1^{trans,Al} = \beta_1^{exp,Ti} + \beta_1^{sim,Al} - \beta_1^{sim,Ti} \tag{3}$$

$$\delta^{exp,Al^2} = \delta^{exp,Ti^2} \tag{4}$$

where β_0, $\beta_1$and δ are the regression parameters associated with the signals. Eq. (4) represents the equality of signal variability.

Here we develop a simplified form of the above quoted (or 'classical') transfer function approach, where the hypothesis of signal linearity is directly used to model the, 'transferred' PoD for related applications. To illustrate this approach, data acquired from extensive experimentation using an austenitic SS specimen is used to predict the PoD curve for similar inspection on identical notch configurations in aluminium components. We assume that the regression parameters are equal in both cases which include the feature of equality of variability in signals as assumed in literature (see [18;21]). Hence, the regression parameters were equated regardless of the material and this is expressed as shown in the following equation,

$$(\beta_0^{trans,Al}, \beta_1^{trans,Al}, \delta^{trans,Al}) = (\beta_0^{exp,SS}, \beta_1^{exp,SS}, \delta^{exp,SS}) \tag{5}$$

where $\beta_0^{trans,Al}$, $\beta_1^{trans,Al}$, $\delta^{trans,Al}$, $\beta_0^{exp,SS}$, $\beta_1^{exp,SS}$ and $\delta^{exp,SS}$ are the regression parameters such as intercept, slope and residual standard deviation of transferred signals for aluminium and experimental signals of SS repectively.

Before performing the regression, the signals were normalized to maintain uniform scale and log transformed for better linearity. The classical signal response PoD function by Berens [3] is based on the relation between defect size and signal response,

$$ln(\hat{a}) = \beta_0 + \beta_1 ln(a) + \delta \tag{6}$$

where 'a' and '$\hat{a}$' are crack length and signal response respectively.

PoD can be determined, for each defect, by calculating the probability of the signal response exceeding the decision threshold, mathematically:

$$PoD(a) = Probability\ (ln(\hat{a}) > ln(\hat{a}_{th})) \tag{7}$$

$$PoD(a) = 1 - \Phi\left[\frac{ln(\hat{a}_{th}) - (\beta_0 + \beta_1 ln(a))}{\sigma_\delta}\right] = \Phi\left[\frac{ln(a) - \frac{(ln(\hat{a}_{th}) - \beta_0)}{\beta_1}}{\left(\frac{\sigma_\delta}{\beta_1}\right)}\right] \tag{8}$$

$$\mu = \frac{(ln(\hat{a}_{th}) - \beta_0)}{\beta_1} \tag{9}$$

$$\sigma = \frac{\sigma_\delta}{\beta_1} \tag{10}$$

where 'Φ' is the cumulative distribution function of normal distribution with mean 'μ' and standard deviation 'σ'.

The crucial parameter in PoD determination is the decision threshold '$\hat{a}_{th}$' and often the signal noise (SN) is considered for determining the decision threshold in signal response PoD analysis: we have also done the same. Since the signals are normalized for uniformity in scale, the measured noise is also normalized. The transferred PoD for aluminium is computed by using the normalized SN in aluminium specimen (NSN^{Al}) as the decision threshold along with the regression parameters of SS experiments. Hence, the mean and variability of transferred PoD are written as,

$$\mu^{trans,Al} = \frac{(\ln(NSN^{Al}) - \beta_0^{exp,SS})}{\beta_1^{exp,SS}} \tag{11}$$

$$\sigma^{trans,Al} = \frac{\delta^{trans,Al}}{\beta_1^{exp,SS}} \tag{12}$$

Thus the transferred PoD for aluminium is computed through a decision threshold based on noise in aluminium, with the linearity parameters of the SS specimen.

4. Results

In order to validate the proposed transfer function approach, the so-transferred PoD is compared with the fully experimentally calculated PoD for the aluminium plate. The comparison of linearity of normalized signals with correspondence to the notch height in both aluminium and SS is shown in Fig. 3 and this gives confidence to our proposed approach. The asymptotic portion of the datasets belonging to larger notch cases was excluded from the analysis. For the studies described in this paper, the decision threshold was chosen to be 15 times that of the amplitude of signal noise measured in experiments (i.e. more than 20 dB). The transferred PoD curve is computed as described in the previous section and it is shown in Fig. 4 along with that obtained using full experimentation on the aluminium sample itself.

The transfer PoD shows good agreement with the experimental PoD

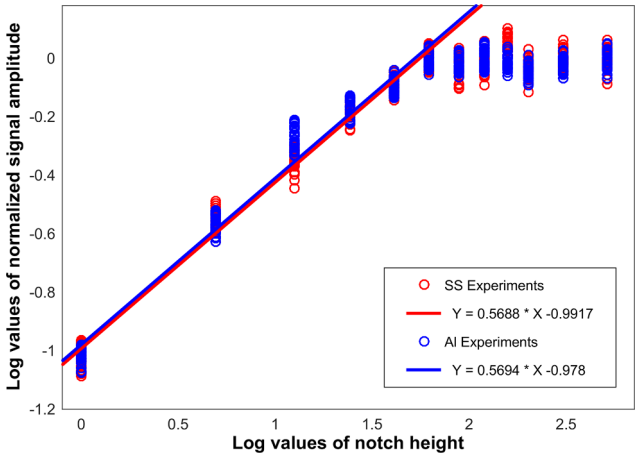

Fig. 3. Linear regression plot of defect response signals obtained as from experiments on stainless steel and aluminium specimens.

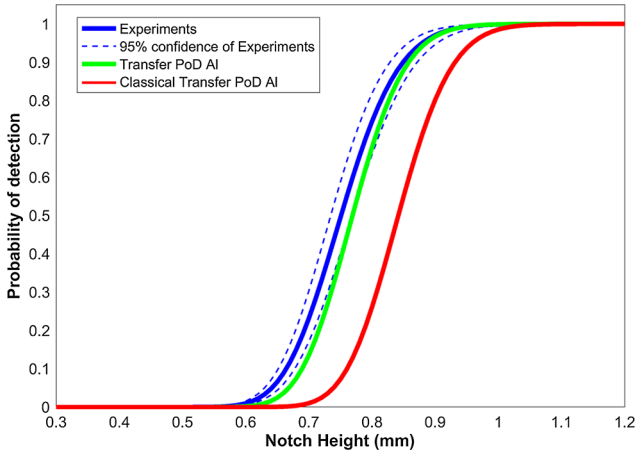

Fig. 4. Comparison of signal noise based transfer PoD of aluminium with full experimental PoD and classical transfer function PoD curves.

curve and it falls within the limits of 95% confidence level of experimental PoD (the 95% confidence level is a widely used metric for characterizing the sampling uncertainty in PoD analysis [2–4]). This gives confidence to the assumptions made in our approach. The classical transfer PoD of aluminium is also computed similar to the work reported in literature [21], for comparison purposes. In order to compute the classical transfer PoD as described in the Eqs. (2)–(4), Finite Element (FE) simulations were carried out for both aluminium and SS specimens. A commercial FE package [30] was used to model the wave propagation assuming 2D plane strain conditions (see our previous work [16] for FE simulation approach and also a justification for using 2D models). The specimen plate was modelled using linear quadrilateral elements. Experimentally measured elastic properties of actual samples were assigned to the models. The integrated probe used in the experiments was modelled as a wedge with Plexiglas properties and its dimensions were extracted from the actual probe used. The boundaries of the domain of interest were modelled by absorbing regions (see [31] for a description of the ALID method used) as shown in Fig. 5 to minimize the wave reflections which helps in identifying the signal of interest. The simulations were performed in a statistical manner by uncertainty propagation in the influential parameters (for detailed description of simulation-supported PoD, see [32–39]). The parameters and the properties used for the models in the FE simulation are given in Table 2 below.

Table 2
Parameters used for Finite Element (FE) model studies of ultrasonic wave-defect interaction.

Sl No	Model Parameter	Aluminium Plate	SS Plate
1	Length of the plate model	75 (mm)	75 (mm)
2	Thickness of plate model	28 (mm)	28 (mm)
3	Material density	2700 (kg/m^3)	8000 (kg/m^3)
4	Young's modulus	70 (GPa)	200 (GPa)
5	Poisson's ratio	0.33	0.29

The comparison of classical transfer function PoD based on [21] with our signal noise based transfer PoD is shown in Fig. 4 and this positively highlights the potential of the present approach in predicting the PoD curves. In addition, the efficacy of the present approach is also demonstrated by computing the transfer PoD contrariwise. The transferred PoD of SS sample is computed by using the experimental data of aluminium sample and it is compared with the classical transfer function PoD and fully experimental PoD for the SS sample. In this case, the decision threshold is based on noise in the SS sample. Fig. 6 shows the comparison of thus transferred PoD of SS sample. In this application also the transferred PoD falls within the limits of the 95% confidence level of experimental PoD curve which shows the potential of this present approach.

5. Discussion

5.1. Defect morphologies

The application of this signal noise based transfer function approach is limited to the scenarios of related defect morphologies in different materials. As failure mechanisms vary with materials, the resulting crack geometries may also vary. The differences in crack geometries in parent and target material can cause variations in signal to noise ratios and on the overall signal and noise behaviour which makes the transfer approach difficult. To emphasize the variation of signal behavior over defect morphologies, simulations of two different cases of branched cracks in SS sample were performed. The considered configurations of

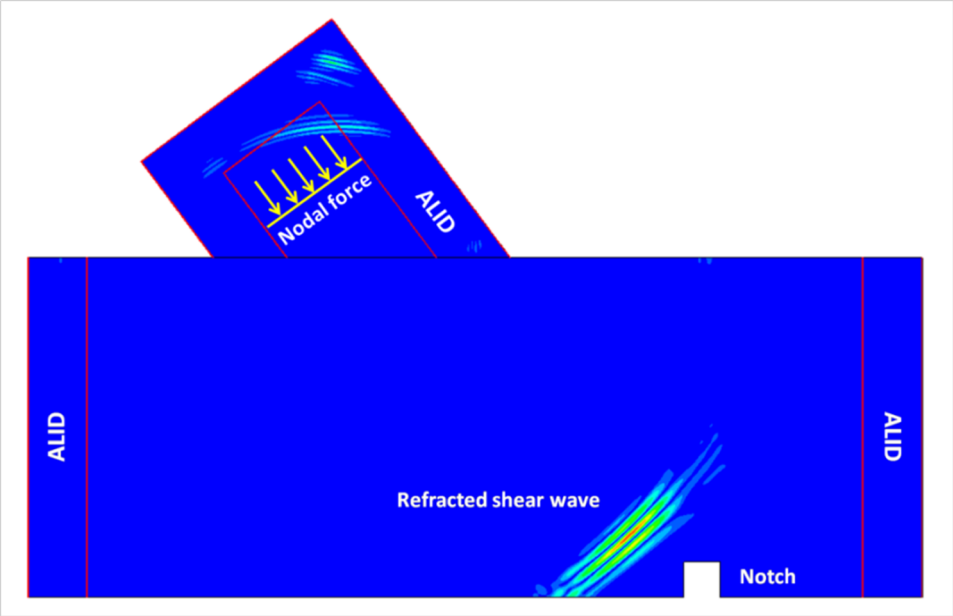

Fig. 5. Schematic of the FE model used for studies in this paper.

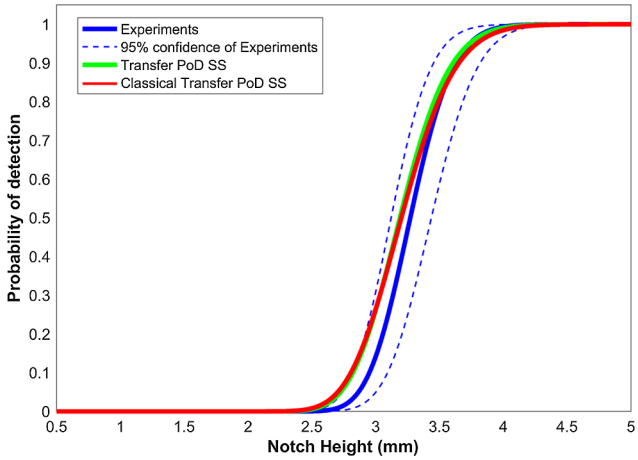

Fig. 6. Comparison of signal noise based transfer PoD of stainless steel with full experimental PoD and classical transfer function PoD curves.

the branched cracks are illustrated in Fig. 7(a) and (b). The type of cracks in Fig. 7(a) has been mainly considered in simulation-based studies in the literature (see for e.g., [40–42]). FE simulations were carried out by simulating the variations in probe position and frequency as similar to simulations discussed in the previous section and 10 runs were performed for each crack case. The normalized scatter plot of the signal amplitudes obtained from simulations are shown in Fig. 8(a) and (b).

It can be observed that the scatter of the normalized signals of 'Y' shape and inclined branched cracks are much different from each other and also they are not similar to the results of EDM notches discussed in the previous section. Thus, target defect morphologies need to be considered in the parent material to establish a linear trend similar to the target defect configuration, since equivalence in linearity is the underlying hypothesis of this approach. This also limits the choice of the parent material to have the feasibility of reproducing the defect morphologies expected in the target material.

5.2. Transfer PoD of SS from MS data

Among the materials considered for demonstrations shown in the previous section, SS has the prevalent failure mechanisms of stress corrosion cracking and intergranular cracking which results in narrow, closed, partially closed and branched type cracks. Although stress corrosion cracking is also reported in aluminium alloys [43–48], in order to further showcase the validity of the approach, another sample specimen made up of MS was considered, where MS can be expected to have failure mechanisms and defect types of the same type as in SS.

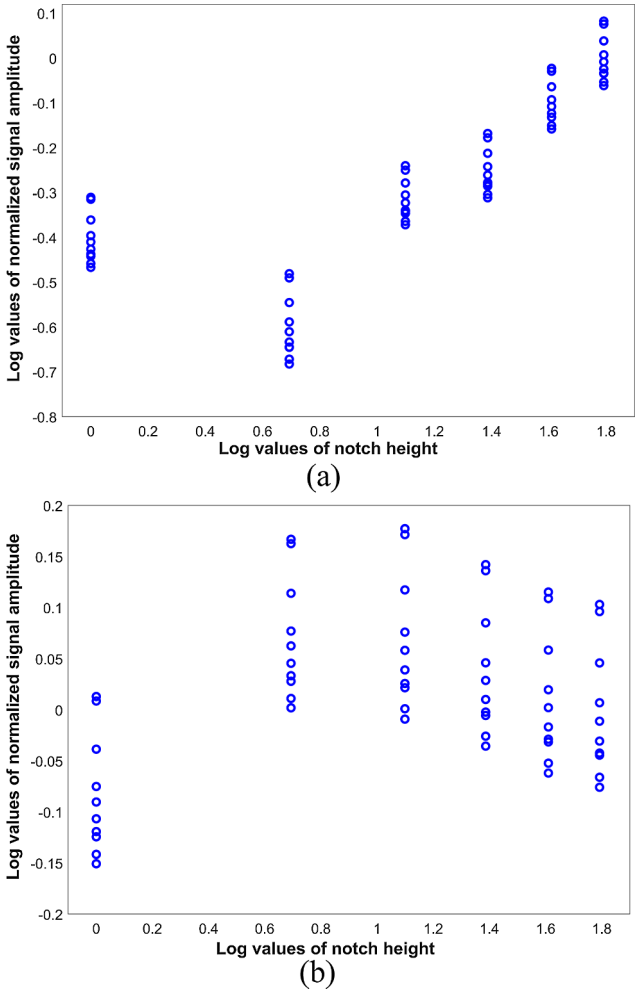

Fig. 8. Scatter plot of the normalized signals obtained from simulations of branched cracks in Stainless Steel (a) 'Y' shape cracks; and (b) inclined branched cracks.

EDM notches of identical configurations as in SS and Al specimens were machined in the MS specimen. Extensive PoD experimental campaign was carried out in a fashion as described in Section 2. The obtained normalized signal amplitude scatter in comparison with the results of SS and Al is shown in Fig. 9 and it further strengthens the underlying hypothesis of the proposed approach.

Transfer PoD curves for SS and Al were computed using the experimental data of MS and also the transfer PoD curve for MS was

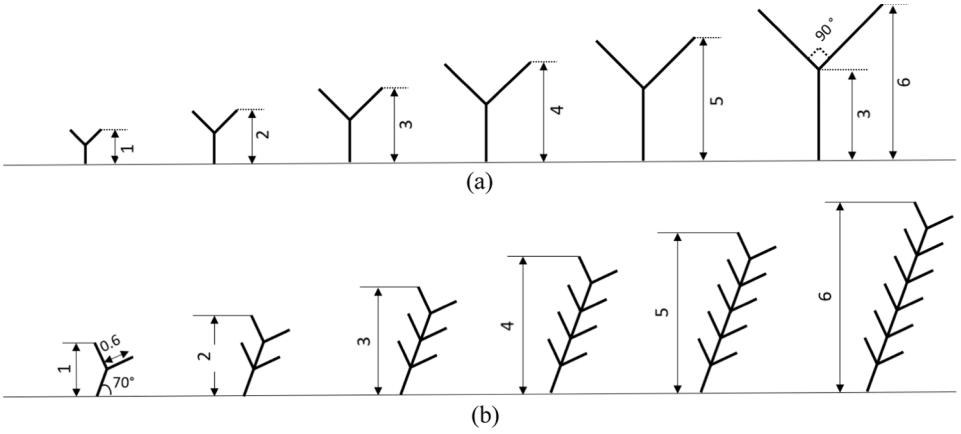

Fig. 7. Schematics of the branched cracks considered for simulations (a) 'Y' shape cracks; and (b) inclined branched cracks. All dimensions are in mm.

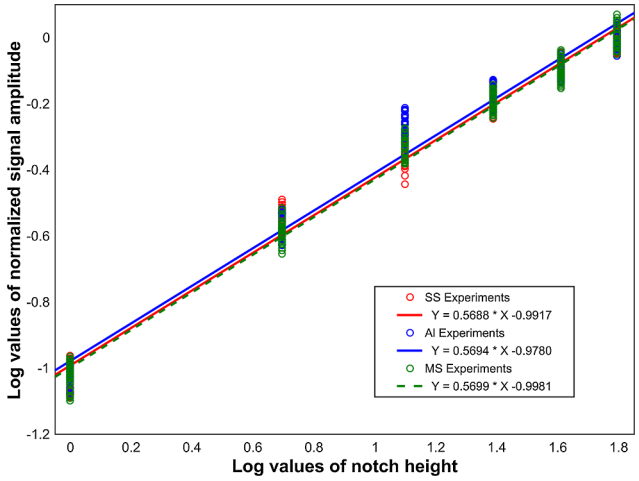

Fig. 9. Linear regression plot of defect response signals obtained as from experiments on mild steel specimen in comparison with results of stainless steel and aluminium specimens.

Table 3
Parameters used for Finite Element (FE) model studies of wave-defect interaction in mild steel specimen.

Sl No	Model Parameter	MS Plate
1	Length of the plate model	75 (mm)
2	Thickness of plate model	28 (mm)
3	Material density	7800 (kg/m^3)
4	Young's modulus	200 (GPa)
5	Poisson's ratio	0.3

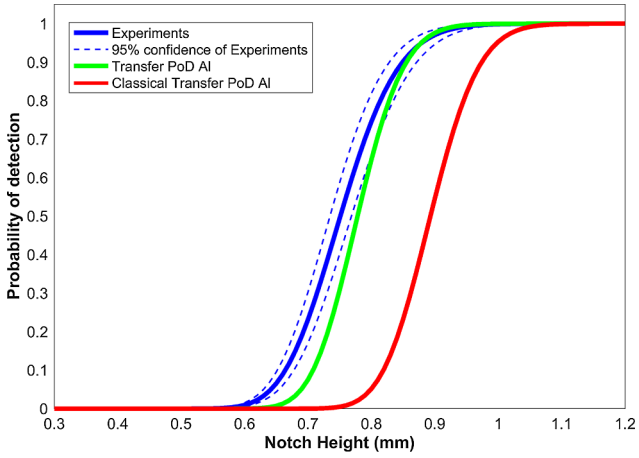

Fig. 10. Comparison of transfer PoD curves of aluminium by using data of mild steel specimen with fully experimental PoD of aluminium.

computed in reverse. Classical transfer PoD curves for respective materials also computed and for this purpose FE simulations for MS specimen were carried out. The parameters used for the FE simulations are listed in Table 3. The computed signal noise based transfer PoD curves in comparison with classical transfer function PoD and experimental PoD are shown in Figs. 10–13.

The comparison of thus computed transfer function PoD curves with fully experimental PoD is quantified in terms of the correlation coefficient and shown in Table 4. For all the cases – SS, aluminium and MS – the signal noise based transfer PoD show very good agreement with the fully empirical PoD. However, the classical transfer function approach requires simulations for both the parent and related application – the accuracy of such models can adversely impact the results. On the other

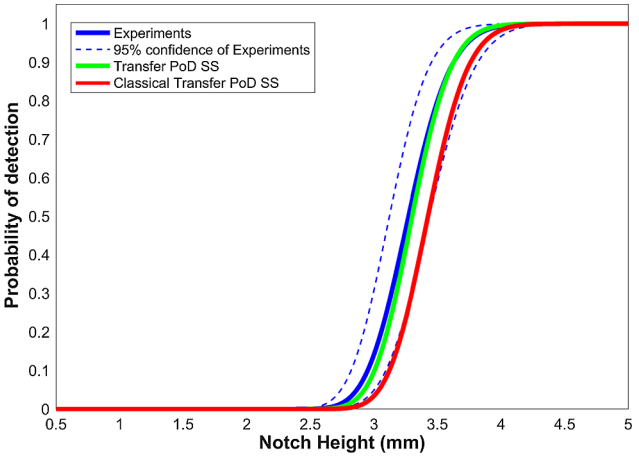

Fig. 11. Comparison of transfer PoD curves of austenitic stainless steel by using data of mild steel specimen with fully experimental PoD of austenitic stainless steel.

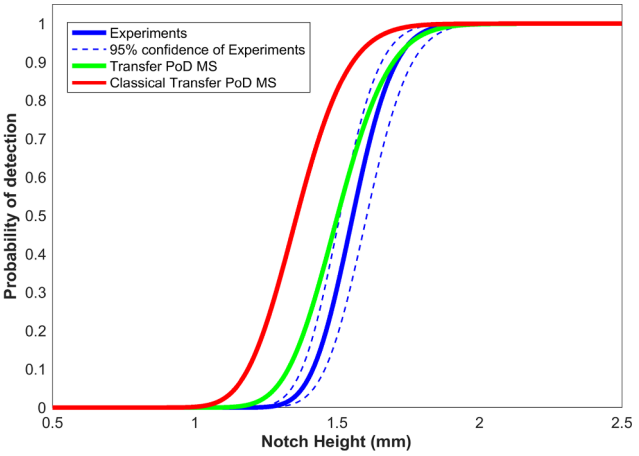

Fig. 12. Comparison of transfer PoD curves of mild steel by using data of aluminium specimen with fully experimental PoD of mild steel.

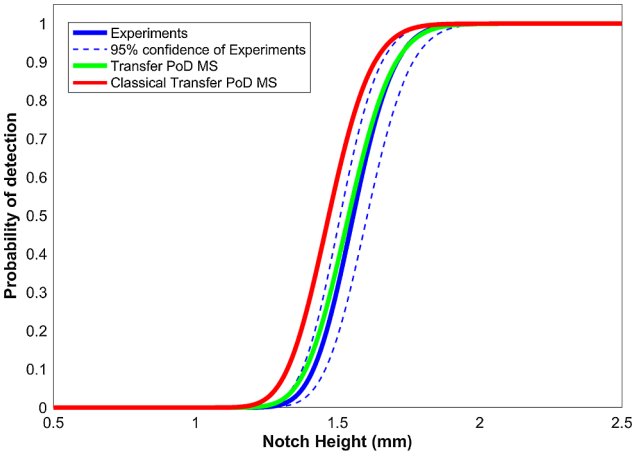

Fig. 13. Comparison of transfer PoD curves of mild steel by using data of austenitic stainless steel specimen with fully experimental PoD of mild steel.

hand, the proposed simplified transfer function approach based on the signal noise requires only the empirical data of the parent application along with the quantified signal noise value in the target application.

One of the limitations of this study is that we have considered only a set of 3 materials, namely Aluminium, SS and MS: however we note,

Table 4
Quantitative comparison of transfer PoD curves with fully empirical PoD curves.

Cases	Experimental data	Classical transfer PoD	Signal noise based transfer PoD
$PoD^{trans,Al}$	SS	0.9778	0.9989
	MS	0.9518	0.9974
$PoD^{trans,SS}$	Al	0.9989	0.9976
	MS	0.9918	0.9996
$PoD^{trans,MS}$	Al	0.9672	0.9971
	SS	0.9926	0.9997

that these are the most widely used metals in engineering applications. Also, in the current implementation, the velocity of the shear ultrasonic mode needs to be similar in the pair of metals chosen, in order to ensure a similar wedge angle for excitation. Indeed, studies of our proposed approach for combinations of more pairs of metallic materials more widely ranging wave velocities are a topic of ongoing research at our group at this time.

Finally, we note here that the goal of this paper is to demonstrate the signal noise based transfer PoD approach rather than computing actual PoD curves. Thus, for simplicity discrete notch heights from 1 mm were considered, whereas the actual PoD estimation requires more number of notches in the transition zone of PoD curve. However, since the approach strongly relies on the equivalence in linearity and closer agreements were observed in all materials having identical notches, inclusion of more notches is not expected to affect the validity of the approach.

6. Conclusion

This paper presented a simplified transfer function approach based on signal noise in the material. The proposed approach was demonstrated through an example case of PoD curve prediction for bulk ultrasonic inspection of a thick aluminium plate by using the empirical PoD data of an otherwise similar austenitic SS plate and a mild steel plate. Similarly, it was also demonstrated in each of the possible combinations among these three materials. The transfer function PoD curve is validated through the comparison with fully empirical PoD curves and results predicted by the classical transfer function PoD curve. Validated 2D FE simulations were used to generate classical transfer function PoD curves. The signal noise based transfer function PoD curves are within the limits of 95% confidence level of extensive experimentation PoD and also shown closer agreements than the classical transfer function PoD. This simplified approach requires only the empirical data of parent application along with the signal noise measurement in the target application. Quantitative comparison in terms of correlation coefficient is also made to show the efficacy of the proposed approach.

The results show the potential of the simplified transfer function approach in predicting PoD curves, however, the application is limited to the scenarios of related defect configurations in different materials. More research is needed to incorporate the effect of variabilities in signal and wider range of defect configurations in diverse materials. In general, the signal noise based transfer function approach is a potential and cost effective tool to transform the PoD data computed for a simple application to a related applications such as materials with different inherent signal noise levels for similar defect types and it can be extended for more complex applications such as inspection of weld defects based on data generated on parent metal.

Funding

This research was supported by the Board of Research in Nuclear Sciences (BRNS), Mumbai, India.

Appendix A. Supplementary material

Supplementary data to this article can be found online at https://doi.org/10.1016/j.ultras.2018.09.015.

References

[1] W. Visser, POD/POS curves for non-destructive examination, Offshore technology report 2000/018: Visser consultancy limited, 3 Valiant road, Weybridge, Surrey KT13932, UK, Online link: www.hse.gov.uk/research/otopdf/2000/oto00018.pdf [Last accessed: September 2018].
[2] C. Annis, MIL-HDBK-1823A, Nondestructive evaluation system reliability assessment, Department of defense handbook, Wright-Patterson AFB, USA, 2009.
[3] A.P. Berens, NDE reliability data analysis quantitative nondestructive evaluation, 8th ed, ASM Metals Handbook,1976, vol. 17, pp. 689–701.
[4] L. Gandossi, C. Annis, Probability of Detection Curves: Statistical Best-Practices, ENIQ TGR Tech Doc 2010; 41, Downloadable from http://bookshop.europa.eu/en/probability-of-detection-curves-pbLDNA24429/ [Last accessed: September 2018].
[5] C. Müller, M. Bertovic, M. Gaal, H. Heidt, M. Pavlovic, M. Rosenthal, K. Takahashi, J. Pitkänen, U. Ronneteg, Progress in Evaluating the Reliability of NDE, Systems – Paradigm Shift. 4th Eur. Work. Reliab. NDE. Berlin, 2009.
[6] M. Pavlović, K. Takahashi, C. Müller, Probability of detection as a function of multiple influencing parameters, Insight – Non-Destructive Test Cond. Monit. 54 (2012) 606–611, https://doi.org/10.1784/insi.2012.54.11.606.
[7] D. Kanzler, C. Müller, J. Pitkänen, Probability of detection for surface-breaking holes with low-frequency eddy current testing a non-linear multi-parametric approach, Insight – Non-Destructive Test Cond. Monit. 56 (2014) 664–668, https://doi.org/10.1784/insi.2014.56.12.664.
[8] N. Yusa, W. Chen, H. Hashizume, Demonstration of probability of detection taking consideration of both the length and the depth of a flaw explicitly, NDT E Int. 81 (2016) 1–8, https://doi.org/10.1016/j.ndteint.2016.03.001.
[9] A. Gianneo, M. Carboni, M. Giglio, Feasibility study of a multi-parameter probability of detection formulation for a Lamb waves–based structural health monitoring approach to light alloy aeronautical plates, SHM 16 (2) (2017) 225–249.
[10] C. Müller, M. Bertovic, D. Kanzler, T. Heckel, M. Rosenthal, R. Holstein, U. Ronneteg, J. Pitkänen, Assessment of the reliability of NDE: a novel insight on influencing factors on POD and human factors in an organizational context, in: 11th Eur. Conf. Non-Destructive Test. Prague, Czech Republic, 2014.
[11] M. Bertovic, M. Gaal, C. Müller, B. Fahlbruch, Investigating human factors in manual ultrasonic testing: testing the human factors model, Insight – Non-Destructive Test. Cond. Monit. 53 (2011) 673–676, https://doi.org/10.1784/insi.2011.53.12.673.
[12] M. Wall, S. Burch, J. Lilley, Human factors in POD modelling and use of trial data, Insight – Non-Destructive Test. Cond. Monit. 51 (2009) 553–561, https://doi.org/10.1784/insi.2009.51.10.553.
[13] M.S. Syed Akbar Ali, P. Rajagopal, Probability of Detection (PoD) curves based on Weibull statistics, J. Nondestruct. Eval. (2018), https://doi.org/10.1007/s10921-018-0468-2 in press.
[14] Online resources, web link: http://www.cnde.iastate.edu/mapod/ [Last accessed: September 2018].
[15] The PICASSO project, web link: http://cordis.europa.eu/result/rcn/140492_en.html [Last accessed: September 2018].
[16] MS Syed Akbar Ali, A. Kumar, P.B. Rao, J. Tammana, K. Balasubramaniam, P. Rajagopal, Bayesian synthesis for simulation-based generation of probability of detection (PoD) curves, Ultrasonics 84 (2018) 210–222, https://doi.org/10.1016/j.ultras.2017.11.004.
[17] K. Smith, PoD transfer function approach, Pratt & Whitney MAPOD Meeting, February 4, 2005.
[18] C.A. Harding, G.R. Hugo, S.J. Bowles, Application of model-assisted POD using a transfer function approach, in: D.O. Thompson, D.E. Chimenti, (Eds.), Rev. Prog. Quant. Nondestruct. Eval. vol. 1096, Chicago (Illinois): AIP Conf. Proc., 2009, pp. 1792–1796.
[19] M. Li, W.Q. Meeker, R.B. Thompson, Physical model-assisted probability of detection of flaws in titanium forgings using ultrasonic nondestructive evaluation, Technometrics 56 (2014) 78–91.
[20] M. Carboni, S.A. Cantini, "Model Assisted Probability of Detection" approach for ultrasonic inspection of railway axles, in: 18th World Conf. Nondestruct. Test. 2012 Conf. Durban, South Africa, 2012, pp. 16–20.
[21] S. Demeyer, F. Jenson, N. Dominguez, E. Iakovleva, Transfer function approach based on simulation results for the determination of pod curves, in: D.O. Thompson, D.E. Chimenti (Eds.), Rev. Prog. Quant. Nondestruct. Eval. AIP Conf. Proc., Burlington, VT, 2012, pp. 1757–1764.
[22] P.N. Bilgunde, L.J. Bond, Temperature compensated transfer function for probability of detection (POD) in high temperature ultrasonic NDE using low temperature signals, in: 10th Int. Top. Meet. Nucl. Plant Instrumentation, Control. Human-Machine Interface Technol. (NPIC HMIT), San Francisco, CA, 2017.
[23] CIVA software from the French Alternative Energies and Atomic Energy Commission or CEA, http://www.extende.com/ [Last accessed: September 2018].
[24] E.P. Papadakis, Revised grain-scattering formulas and tables, J. Acoust. Soc. Am. 37 (1965) 703–710, https://doi.org/10.1121/1.1909399.
[25] A. Eriksson, J. Whittle, ENIQ Recommended Practice 1, Influential/Essential

Parameters, Issue 2. ENIQ report 24, 2005. http://s538600174.onlinehome.fr/nugenia/wp-content/uploads/2014/02/RP1-INFLUENTIAL_ESSENTIAL_PARAMETERS_ISSUE-2.pdf [Last accessed: September 2018].
[26] Integrated angle beam probe. Product description available in http://www.eecindia.com/ wp-content/uploads/2017/07/PROBES.pdf [Last accessed: September 2018].
[27] RITEC RPR-4000 pulser receiver, Product details available in http://www.ritecinc.com/pdfs/rpr4000specs.pdf [Last accessed: September 2018].
[28] Keysight technologies DSOX3024T Oscilloscope, Product details available in http://www.keysight.com/en/pdx-x202173-pn-DSOX3024T/oscilloscope-200-mhz-4-analog-channels?cc=IN&lc=eng [Last accessed: September 2018].
[29] R. Hogg, Probability and Statistical Inference, 9th ed., Pearson, Upper Saddle River, New Jersey, 2015.
[30] ABAQUS 6.9 user's manual, http://130.149.89.49:2080/v6.9/index.html [Last accessed: September 2018].
[31] P. Rajagopal, M. Drozdz, E.A. Skelton, M.J.S. Lowe, R.V. Craster, On the use of absorbing layers to simulate the propagation of elastic waves in unbounded isotropic media using commercially available finite element packages, NDT E Int. 51 (2012) 30–40.
[32] B. Chapuis, P. Calmon, Jenson F. Best, Practices for the Use of Simulation in POD Curves Estimation: Application to UT Weld Inspection, Springer International Publishing, 2017.
[33] S.M. Subair, S. Agrawal, K. Balasubramaniam, P. Rajagopal, A. Kumar, P.B. Rao, On a framework for generating PoD curves assisted by numerical simulations, in: D.E. Chimenti, L.J. Bond (Eds.), Rev. Prog. Quant. Nondestruct. Eval. AIP Conf. Proc., Boise, Idaho, 2015, pp. 1907–1914.
[34] S.M. Subair, K. Balasubramaniam, P. Rajagopal, A. Kumar, B.P.C. Rao, T. Jayakumar, Finite element simulations to predict probability of detection (PoD) curves for ultrasonic inspection of nuclear components, Proc. Eng. 86 (2014) 461–468, https://doi.org/10.1016/j.proeng.2014.11.059.
[35] H. Wirdelius, G. Persson, Simulation based validation of the detection capacity of an ultrasonic inspection procedure, Int. J. Fatigue 41 (2012) 23–29.
[36] B. Chapuis, F. Jenson, P. Calmon, G. DiCrisci, J. Hamilton, L. Pomie, Simulation supported POD curves for automated ultrasonic testing of pipeline girth welds, Weld World 58 (2014) 433–441.
[37] N. Dominguez, F. Reverdy, F. Jenson, POD evaluation using simulation: a phased array UT case on a complex geometry part, in: D.O. Thompson, D.E. Chimenti (Eds.), Rev. Prog. Quant. Nondestruct. Eval. AIP Conf. Proc., Baltimore, Maryland, USA, 2014, pp. 2031–2038.
[38] G. Ribay, X. Artusi, F. Jenson, C. Reece, P.-E. Lhuillier, Model-based POD study of manual ultrasound inspection and sensitivity analysis using metamodel, in: D.O. Thompson, D.E. Chimenti (Eds.), Rev. Prog. Quant. Nondestruct. Eval. AIP Conf. Proc., Minneapolis, Minnesota, 2016, p. 200006.
[39] V.K. Rentala, P. Mylavarapu, J.P. Gautam, Issues in estimating probability of detection of NDT techniques – a model assisted approach, Ultrasonics 87 (2018) 59–70, https://doi.org/10.1016/j.ultras.2018.02.012.
[40] J.D. Achenbach, K.Y. Hu, A.N. Norris, T.A. Gray, R.B. Thompson, A model for the ultrasonic scattering from multi-branched cracks, in: D.O. Thompson, D.E. Chimenti (Eds.), Rev. Prog. Quant. Nondestruct. Eval. Springer, California, San Diego, 1985, pp. 91–102.
[41] S. Mahaut, N. Leymarie, C. Poidevin, T. Fouquet, O. Dupond, Study of complex ultrasonic NDT cases using hybrid simulation method and experimental validations, Insight 53 (12) (2011) 664–667, https://doi.org/10.1784/insi.2011.53.12.664.
[42] M.V. Felice, A. Velichko, P.D. Wilcox, T. Barden, T. Dunhill, Obtaining geometries of real cracks and using an efficient finite element method to simulate their ultrasonic array response, Insight 56 (9) (2014) 492–498, https://doi.org/10.1784/insi.2014.56.9.492.
[43] A.C.U. Rao, V. Vasu, M. Govindaraju, Kvsai Srinadh, Stress corrosion cracking behaviour of 7xxx aluminum alloys: a literature review, Trans Nonferrous Met. Soc. China 26 (2016) 1447–1471, https://doi.org/10.1016/S1003-6326(16)64220-6.
[44] M.O. Speidel, Stress corrosion cracking of aluminum alloys, Metall Trans. A 6 (1975) 631, https://doi.org/10.1007/BF02672284.
[45] M.B. Kannan, P.B. Srinivasan, V.S. Raja, 8 – Stress corrosion cracking (SCC) of aluminium alloys, in: V.S. Raja, T. Shoji (Eds.), Stress Corros. Crack. Woodhead Publishing, 2011, pp. 307–340 https://doi.org/10.1533/9780857093769.3.307.
[46] L. Burnett Timothy, N.J. Henry Holroyd, M. Scamans Geoffrey, Xiaorong Zhou, E. Thompson George, J. Withers Philip, The role of crack branching in stress corrosion cracking of aluminium alloys, Corros. Rev. 33 (2015) 443, https://doi.org/10.1515/corrrev-2015-0050.
[47] D.J. Seguin, Intergranular Corrosion and Stress Corrosion Cracking of Extruded AA6005A, Michigan Technological University, 2013.
[48] D.P. Field, H. Weiland, K. Kunze, Intergranular cracking in aluminum alloys, Can. Metall. Q 34 (1995) 203–210, https://doi.org/10.1016/0008-4433(95)00002-F.